Int. J. Environ. Sci. Technol. (2015) 12:3685–3694
DOI 10.1007/s13762-015-0810-5

ORIGINAL PAPER

Selective recovery of chromium ions from waste tannery solution for preparation of chromium oxide nanoparticles

S. M. El-Sheikh[1] · **M. A. Rabah**[2]

Received: 28 February 2013 / Revised: 28 January 2015 / Accepted: 17 March 2015 / Published online: 9 April 2015

Abstract This investigation seeks to reduce the environmental impact of the tanning process by recovering Ca and Cr from tannery waste solution. The treatment process reduces both the amount of Cr discharged to the environment and the amount of raw Cr extracted from natural resources. The procedure was based on the selective separation of Ca ions from the waste solution as Ca oxalate, prior to the recovery of Cr as the hydroxide precipitate at pH 6.5. The dried Cr hydroxide cake was then subjected to heating (heating rate 0.5 °C min^{-1}) at different temperatures up to 500 °C to produce Cr oxide nanoparticles. The physicochemical characteristics of the nanoparticles were investigated using X-ray diffraction, Fourier transform infrared, scanning electron microscopy, transmission electron microscopy, surface area measurement and thermal analysis. Results revealed that heating of the treated Cr hydroxide at 300 °C yielded amorphous Cr oxide, while with heating at 400 °C, the Cr oxide started to crystallize to hexavalent, trivalent and divalent Cr species. At 500 °C, a pure phase consisting of trivalent Cr oxide nanoparticles was formed that contained traces of hexavalent Cr. A mechanism for the formation of the different forms of Cr oxide was proposed and confirmed by XRD.

Keywords Nanomaterials · Secondary resources · Selective separation · Chromium oxide nanoparticles

Introduction

In leather tanning, various salts and lime are used in the early stages of the process. Chromium sulfate is widely used as a tanning agent. Traditional leather tanning operations discharge about 42 % of the input chromium (Cr) as a waste solution (Ludvik 2004). High efficiency in the tanning process and recycling of the Cr cannot completely eliminate Cr from the wastewater, given that there is usually significant discharge in post-tanning processes (IULTCS 2014). Chromium exists in different chemical forms, most commonly the trivalent [Cr(III)] and hexavalent [Cr(VI)] forms. The trivalent form of Cr is non-toxic and relatively immobile in nature, whereas hexavalent Cr is readily soluble in water, highly toxic and mobile, and is known to be toxic with potential carcinogenic effects (Gebrehawaria et al. 2014; Jiao et al. 2014). Recovery of Cr from waste tannery solutions has been studied using various physicochemical processes, such as oxidation/reduction, precipitation/filtration, coagulation, ion exchange, adsorption and membrane separation. Kanagaraj et al. (2008) reported that the water extract from the bark of the tree species, Acacia mollissima, was used for recovery of Cr from tannery waste water at different pH values (7, 8 and 9). The recovered Cr was reused for tanning pelts. Moreover, plant-derived biosurfactant quillaja bark saponin was applied to a dewatered tannery sludge for Cr recovery, and a comparative assessment with an H_2O_2 oxidative treatment method was undertaken (Kilic et al. 2011). The H_2O_2 treatment, which involved oxidation of Cr(III)–Cr(VI) and extraction with sulfuric acid solution at

---

✉ S. M. El-Sheikh
selsheikh2001@gmail.com

[1] Nanostructured Materials Division, Advanced Materials Department, Central Metallurgical R and D Institute (CMRDI), P.O. Box 78, Helwan, Cairo 11421, Egypt

[2] Electrochemical and Chemical Treatment Laboratory, Minerals Department, Central Metallurgical R and D Institute (CMRDI), P.O. Box 78, Helwan, Cairo 11421, Egypt

pH 2, enabled the extraction of 70 % of Cr within 4 h at room temperature (Kilic et al. 2011). Furthermore, Tahir et al. (2007) reported that more than 99 % of Cr(III) from tannery wastewater (3 M sulfuric acid) was recovered by adsorption onto bentonite clay. In addition, batch and column experiments using biological waste material (sawdust, rice husk, coir pith and charcoal) and a naturally occurring mineral (vermiculite) have been tested for their effectiveness in removing Cr from tannery effluent. The biosorbent and mineral vermiculite in column format were found to be very effective in removing Cr from tannery effluent (Sumathi et al. 2005). Meanwhile, Ortega et al. used a nanofiltration membrane to separate NaCl and $Cr_2(SO_4)_3 \cdot 5H_2O$ from tannery effluents. These workers demonstrated that Cr(III) retention was dependent on the membrane type used, the Cr^{3+} concentrations (15.2 and 30.3 molm^{-3}) and the operating conditions (Ortega et al. 2005). Additional methods for recovery of Cr from tannery waste solutions have been proposed, including separation of Cr(III) by oxidation to Cr(VI) with sulfuric acid (Macchi et al. 1991) and bio-leaching using a novel mixture of iron- and sulfur-oxidizing bacteria (Zhou et al. 2006), as well as ion exchange (Kabir et al. 2008). The main drawbacks of these methods are operational difficulties, excessive use of chemicals and long processing times. Recently, Abreu et al. (2009) reported that the Cr oxide extracted from Cr-rich waste sludge could serve as a ceramic pigment in a conventional glaze composition usually used in the ceramic tile industry. Moreover, Cr oxide, synthesized by thermal decomposition of solid precursors, was evaluated as a catalyst for ammonia decomposition (Zhu et al. 2008). El-Sheikh et al. (2009a, b) and El-Sheikh and Rabbah (2013) reported that the amorphous phase of Cr_2O_3, which formed at room temperature, was transformed to the crystalline phase by heat treatment at about 400 °C.

A coagulating agent is typically used for solids separation in wastewater treatment, and aluminum (Al) salts such as $Al_2(SO_4)_3$ and $AlCl_3$ are generally used for this purpose. In solution, the Al ion hydrolyzes and generates some ionic monomer species like $Al(OH)_4^-$, $Al(OH)_2^+$ and $Al(OH)^{2+}$, and also polymeric species like $Al_{13}O_4(OH)_{24}^{7+}$, as well as $Al(OH)_3$. The interaction of these species with wastewater contaminants leads to the aggregation of colloidal particles, which later precipitate (Song et al. 2004). The precipitated portion, defined as primary sludge, is then separated from the clear effluent. This process is clearly efficient for removing wastewater contaminants and, as noted by Cañizares et al. (2006), is basically a simple physicochemical process of phase transfer.

To date, no studies have been reported on the selective removal of calcium (Ca) ions before precipitation of Cr ions from industrial waste tannery solutions. In this study, an investigation has been made to recover Cr from spent tannery liquor by a simple separation technique based on precipitation. A key research objective was to separate Ca and Cr before preparation of trivalent Cr oxide nanoparticles. A further objective was to clean the wastewater prior to recycling and reuse in the tanning process.

Materials and methods

Reagents and materials

Approximately 2 m^3 of waste tannery solution was supplied by a tannery plant located at El-Basaten in Cairo. Analytical grade oxalic acid (99.8 %, Brixworth, Northampton, UK), ammonium chloride (99.7 %, RPS Chemical Co. Ltd, Lutterworth, UK), ammonium hydroxide (25 %, ADWIC, Cairo, Egypt), petroleum ether and ethyl ether (99.8 % ADWIC, Cairo, Egypt) were used without further purification. Doubly distilled water was used for chemical analysis and the rinsing and washing of laboratory ware.

Methods

The waste tannery solution was filtered using a cloth silk screen (Nr. 1000, Switzerland). The solids collected on the filter were discarded. A sample of the filtrate was dried in a laboratory oven maintained at 105 °C. Fifteen grams of the dried solid was ground and analyzed by X-ray fluorescence (XRF). A further portion of filtrate was stirred with a mixture of one part petroleum ether and one part ethyl ether for 6 h at room temperature to attain partial removal of the soluble fats. The degreased solution was separated from the organic solvents with a separating funnel. Organic solvents were recycled. Calcium ions were removed from a sample of the waste solution by precipitation as Ca oxalate at room temperature and 70 °C over 1 h. The filtrate was then taken for further processing. Precipitation of Cr as the hydroxide was carried out by the addition of a few milliliters of ammonia solution preceded by ammonium chloride as a buffer salt. Addition of ammonia was carried out dropwise to attain a pH value of 6.5 compared with pH 3.3 for the original waste solution. The precipitate was dried at 105 °C. The dried precipitate was washed with hot water several times to remove sodium chloride. The precipitate was then heated at various temperatures between 300 and 500 °C for 2 h, using a clean porcelain crucible. Heating was performed in a muffle furnace (type Nabertherm, Netherlands), equipped with an automatic temperature controller. Temperature was increased at a rate of 0.5 °C min^{-1}, starting from room temperature. Throughout the process of metals separation, the wastewater was purified using a 0.005 % solution of polyacrylamide (PA)

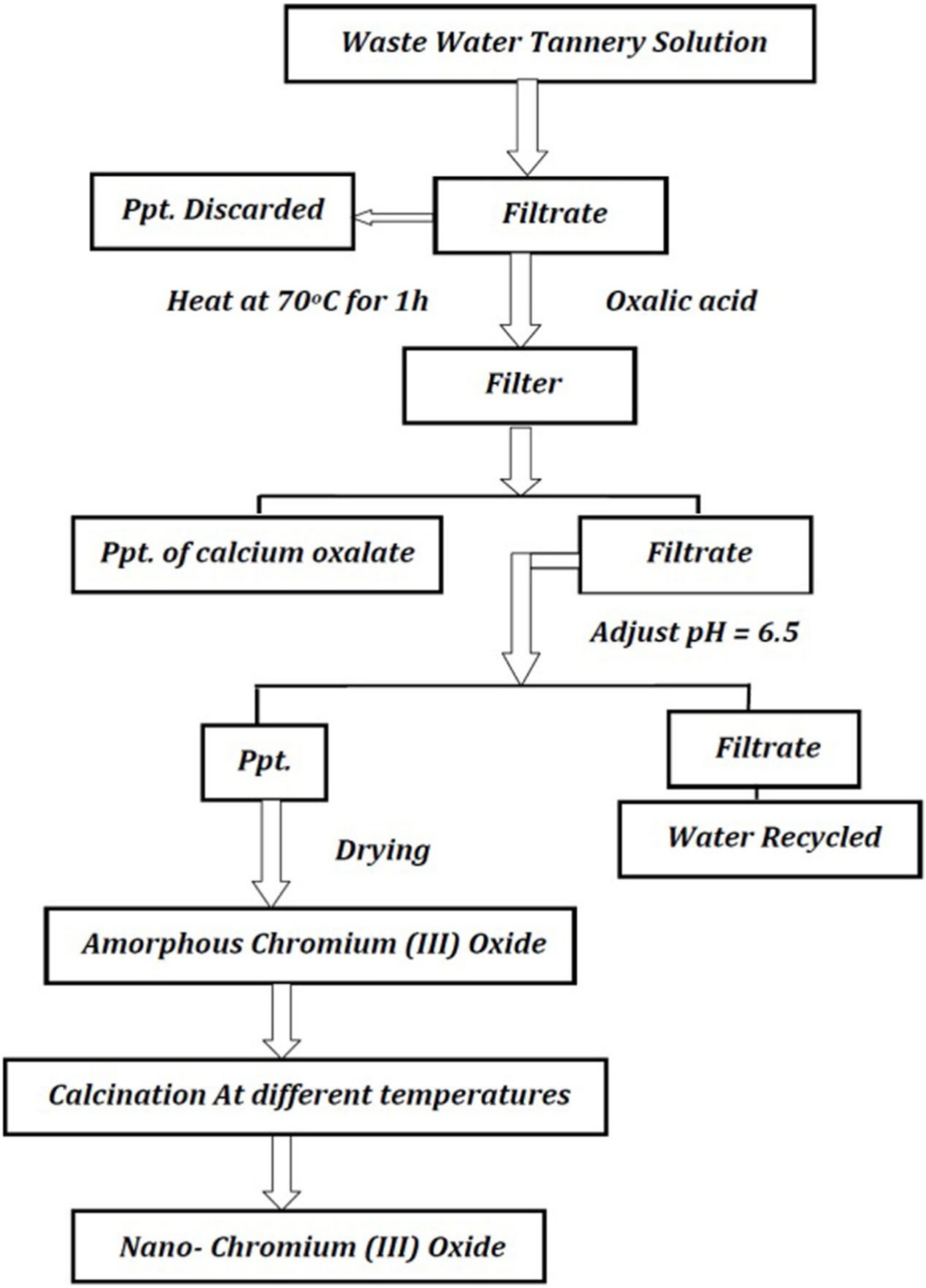

Fig. 1 Schematic diagram for synthesis of chromium oxide nanoparticles from tannery waste solution

(100 Cyanamid, France), as coagulant. The filtered water was suitable for reuse. Figure 1 shows a schematic diagram of the process followed for the preparation of Cr oxide from the waste solution.

Nanoparticle characterization

Instrumentation

A laser ablation system (UP213 New Wave) interfaced to an inductively coupled plasma mass spectrometer [ICP-MS, Varian (Brucker), LA, USA] was used for trace analysis of the fine metal powder. A sequential WD-XRF (Axios, Panalytical 2005, Almelo, Netherlands) was used to determine major and minor components (Beckhoff et al. 2006) in the powder. Phase identification, purity, relative crystallinity and crystal size measurements on the prepared compounds were performed at room temperature with the aid of XRD (Bruker AXIS D8, Germany) with Cu-K_α ($\lambda = 1.5406$ Å, radiation and secondary monochromator 2θ in the range of 20°–80°). The relative crystallinity and crystal size were calculated via the Scherrer equation (Scherrer 1918; Patterson 1939). Transmission electron microscopy (TEM, JEOL-JEM-1230, Tokyo, Japan) was used to determine the microstructure of the Cr oxide samples (Williams et al. 1996). Infrared absorption spectroscopy (IR) was performed with a JASCO 3600 IR spectrophotometer (Tokyo, Japan). A scanning electron microscope (SEM, JEOL model JSM-5410, Tokyo, Japan) was used to investigate the microstructure of the prepared material end product.

Specific surface area

The specific surface area, pore volume and pore size distribution of samples heated at 400 °C were measured using the nitrogen adsorption–desorption technique (Quantachrome, model NOVA 2000). The sample was degassed at 373 K for 24 h before measurement at 77 K. The adsorbed gas volume was taken as cm^3 per g at STP. The pore size was calculated from the desorption isotherms based on the Barrett, Joyner and Halenda (BJH) method (Terzyk et al. 2007). The BJH method is a procedure for calculating pore size distributions from experimental isotherms using the Kelvin model of pore filling and applies only to the mesopore and small macropore size ranges. The specific surface area was calculated using the Brunauer–Emmett–Teller equation (BET) (Brunauer et al. 1938).

Thermal analysis

Thermogravimetric (TGA) and differential thermogravimetric (DTA) analyses were performed by heating the sample at a rate of 10 °C/min using a Shimadzu-50H TGA analyzer (Tokyo, Japan) in an air atmosphere (Coats et al. 1963).

Results and discussion

Effect of pH on Cr precipitation

Measurement of sample pH indicated that the waste solution was slightly acidic with a pH of 3.3. Figure 2 shows the effect of pH on the precipitation of Cr hydroxide. With an increase in pH from 3.3 to 10, two plateau levels are evident. The first plateau at pH 6.5 represents the precipitation of Cr hydroxide, while the second plateau at pH 8.5 is assigned to the precipitation of Mg hydroxide.

The effect of temperature on weight loss

Figure 3 shows the weight loss from the gel-like precipitate as a result of heating at 80 and 100 °C. It is seen that with an increase in the time of heating from 80 and 100 °C there is a corresponding increase in the weight loss. It is suggested that for the early period of heating, the weight loss was due to the removal of water present in the gel. After 8 h of heating at 100 °C, the weight loss amounted to 65 %. With further heating for 24 h, the weight loss approached a relatively constant value of 92 %, yielding a salt composition of 8 % w/w (dry weight basis).

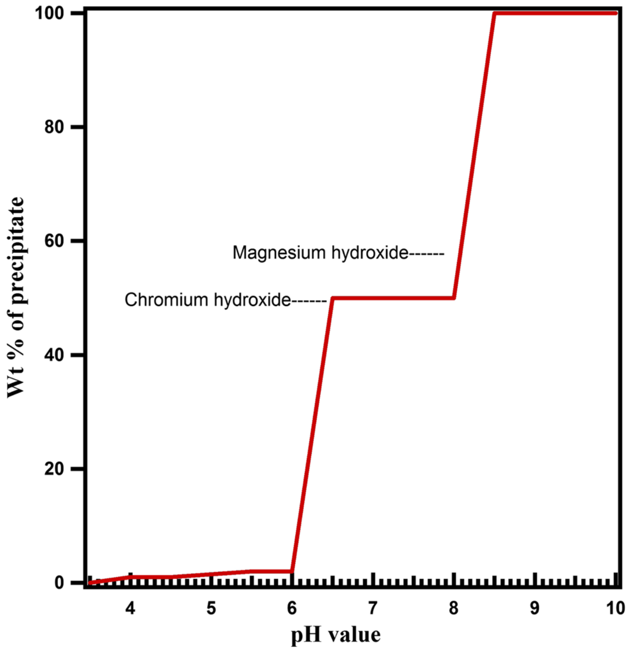

Fig. 2 Effect of pH on precipitation of chromium and magnesium hydroxide (El-Sheikh and Rabbah 2013)

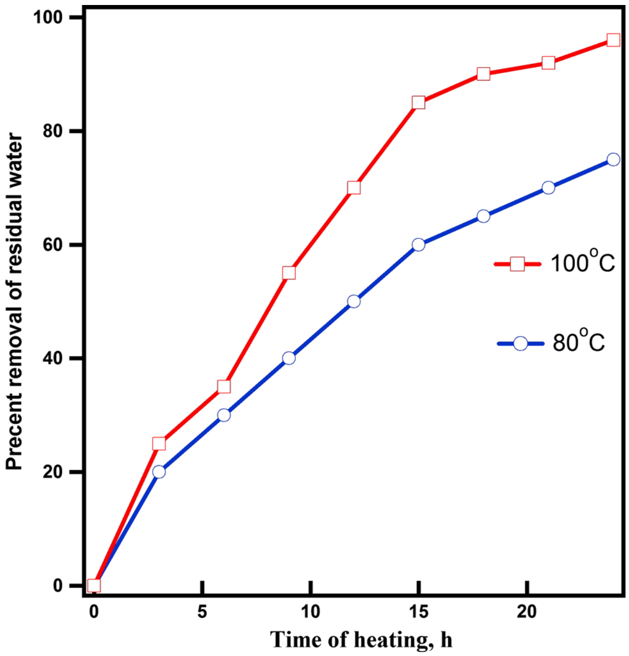

Fig. 3 Weight loss for Cr (OH)$_3$ gel as affected by temperature and time (El-Sheikh and Rabbah 2013)

Table 1 Solids present in the tannery waste solution as revealed by XRF (El-Sheikh and Rabbah 2013)

Compound	Weight %	Compound	wt%
Na as Na_2O	29.122	NaCl	74.958
Mg as MgO	3.292	$MgSO_4$	9.820
Ca as CaO	2.798	$Ca(OH)_2$	3.697
Cr as Cr_2O_3	3.125	$Cr_2(SO_4)_3$	9.007
K as K_2O	0.920	KCl	1.096
Al as Al_2O_3	0.094	$AlSO_4$	0.138
Si as SiO_2	0.259	SiO_2	0.259
P as P_2O_5	0.034	P_2O_5	0.166
Fe as Fe_2O_3	0.058	Fe_2O_3	0.058
Zn as ZnO	0.019	$ZnSO_4$	0.042
Sr as SrO	0.020	SrO	0.020
Cl	38.62	others	0.739
SO_4	21.562		
Br	0.077		
	100 %		100 %

XRF analysis

Table 1 shows the XRF data for the inorganic components derived from the tannery waste solution. Sodium chloride is the major component (75.0 wt%) of the powdered precipitate. Chromium sulfate (9.00 %), Mg sulfate (9.82 %) and Ca hydroxide (3.70 wt%) were also measured. Other salts were present at the trace level.

XRD of Ca oxalate

Figure 4 shows the XRD patterns for Ca oxalate and Ca sulfate precipitated by addition of oxalic acid at room temperature and at 70 °C, respectively. Sharp XRD peaks for Ca oxalate were obtained at room temperature. The peaks were prominent and consisted of two different phases of Ca oxalate: The first phase (141) was tetragonal weddellite (JCPDS card no. 75-1314) and the other phase (040) was monoclinic weddellite (JCPDS card no. 75-1313). In the case of Ca sulfate, this was formed as a result of the reaction of sulfate ions, present in the filtrate, with the oxalate salt to give a thermally stable compound (JCPDS card no. 74-1433).

XRD of Cr oxide

Figure 5 shows the XRD patterns of the Cr_2O_3 nanoparticles produced by precipitating Cr hydroxide at pH 6.5 and heating at various temperatures (300, 400 and 500 °C). The soaking time was 3 h with a heating rate of 0.5 °C/min. Spectra are presented as multiple plots. It can be seen that for the sample heated at 300 °C, Cr has an amorphous phase. The XRD pattern of the powdered sample heated at 400 °C shows several prominent XRD peaks. The material consisted of two different phases of Cr oxide. One was Cr_2O_3 (JCPDS card no. 82-1484) and the other phase was CrO_3 (JCPDS card no. 01-0622). With further increases in temperature up to 500 °C, the stable crystalline hexagonal (rhombohedral) form of the Cr_2O_3 phase developed, the material containing traces of CrO_3. Peak intensities slightly increased with increasing calcination temperature. These findings are in good agreement with published studies (Gupta et al. 2014; Colmenares et al. 2014).

Crystallite size of Cr oxide measured by XRD

Calculation of the crystallite size from the XRD data using the Scherrer equation revealed that the crystallite size increased with increasing temperature. For example, the crystallite size increased from 60 to 80 nm as the calcination temperature increased from 400 to 500 °C. This phenomenon is attributed to the fact that increasing temperatures confer an enhanced tendency for particle grain growth.

FT-IR spectra

The IR spectra of Cr_2O_3 powders obtained from precipitated Cr hydroxide at pH 6.5 and for heating at various temperatures (300, 400 and 500 °C) are presented in Fig. 6. The spectra display bands at 404–414, 563–566, 623, 880, 1097–1145 and 1619 cm^{-1} as well as a broad band

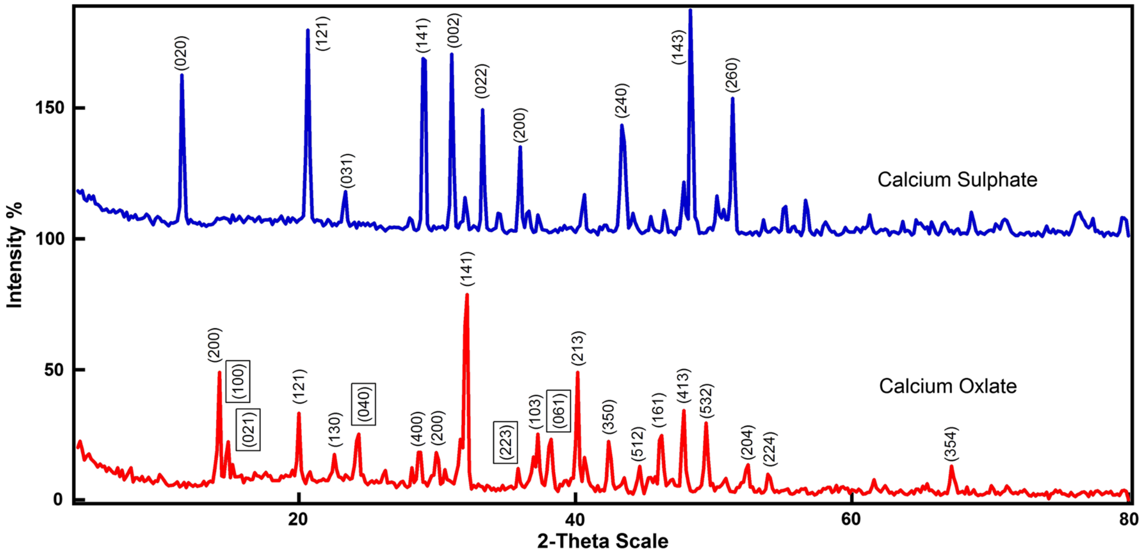

Fig. 4 XRD pattern of calcium oxalate and sulfate precipitated by the addition of oxalic acid at room temperature (RT) and at 70 °C, respectively

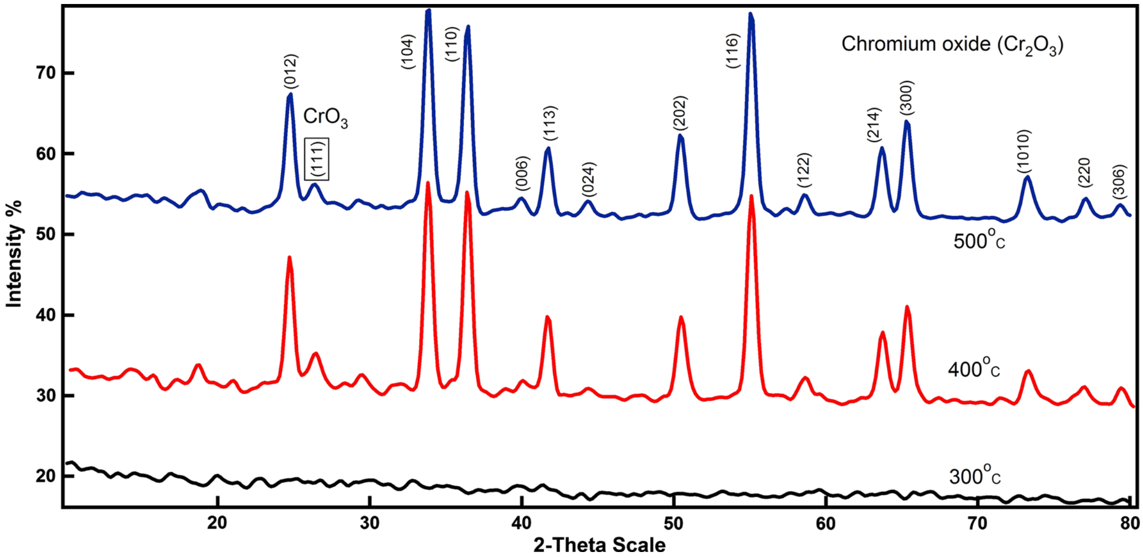

Fig. 5 XRD patterns for Cr_2O_3 nanoparticles after heating chromium hydroxide samples (pH 6.5) to various temperatures (300, 400 and 500 °C)

between 2800 and 3366 cm^{-1}. It can be deduced that the appearance of the latter band is ascribed to the surface −(OH) stretching groups resulting from a dissociation of chemisorbed and non-dissociated water molecules (El-Sheikh et al. 2009a; Lime et al. 2006). The weak absorption bands appearing at 1619 and the strong peak at 1097–1145 cm^{-1} are attributed to hydroxyl groups associated with Cr^{3+} ions. The large band in the range 400–650 cm^{-1} may be assigned to the bonds between Cr and oxygen atoms. The strong sharp peak at 563–566 cm^{-1} was attributed to hexagonal Cr_2O_3 and corresponded to the characteristic vibrational mode of symmetric octahedral CrO_6 of Cr_2O_6. The strong sharp peak that appeared at 880 cm^{-1} was ascribed to Cr_2O_3 (El-Sheikh et al. 2009a; Lime et al. 2006). The FT-IR analysis with sample heated at 300 °C revealed a prominent broadband in the region 3688–2850 cm^{-1} and bands at 544, 755, 943 and 1104 cm^{-1}. The band at 943 cm^{-1} gradually disappeared with increase in temperature. This result is consistent with the transition of amorphous Cr_2O_{3+x} to crystalline Cr_2O_3 (El-Sheikh et al. 2009a; Lime et al. 2006). This conclusion is also consistent with the XRD data.

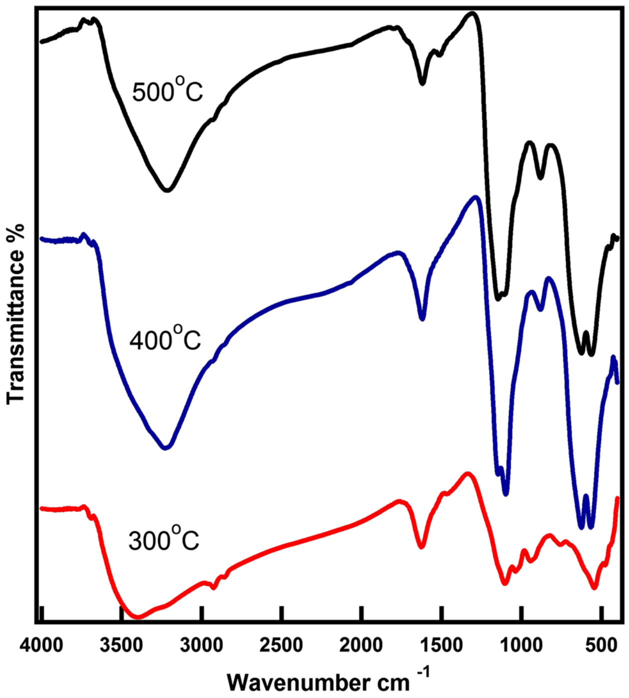

Fig. 6 FT-IR spectra (400–4000 cm^{-1}) of Cr_2O_3 nanoparticles precipitated at pH 6.5 and heated at different temperatures

Morphology of Cr oxide

The SEM image of the Cr oxide powder after heating at 500 °C is presented in Fig. 7a. It can be seen that the sample consisted of spherical particles uniformly distributed. The TEM images of the Cr oxide sample, after heating at 400 and 500 °C as shown in Fig. 7 b–e, reveal particles of diameter 80–400 nm. Additionally, Fig. 7c clearly shows that the microsphere structure is an assemblage of smaller nanoparticles. Figure 7e, d indicates that Cr_2O_3 particles have a mesospheric structure after being heated at 500 °C. This is attributed to the fact that small nanoparticles possess a large specific surface area and would be active catalytic centers able to form microspheres. Meanwhile, the average crystallite size increased with an increase in the heating temperatures from 400 to 500 °C.

Specific surface area

Results for the specific surface area of Cr oxide and the pore diameter for a sample heated at 400 °C are presented in Fig. 8a and b. It is seen that the Cr_2O_3 nanopowder has a surface area of 30 m^2 g^{-1}. The isotherm type for the Cr oxide is type IV according to the IUPAC classification. This category exhibits the characteristic hysteresis loop of mesoporous materials (El-Sheikh et al. 487, 2009b) and confirms that nanosize Cr oxide obtained by thermal treatment has a mesoporous structure. This is consistent with the fully dispersed collagen proteins in the gel precipitate undergoing thermal decomposition with the empty space in effect becoming a framework of pore voids. The adsorption–desorption isotherm of Cr oxide samples at partial pressures of P/Po 0.4–0.84 shows a large hysteresis loop owing to capillary condensation in the mesoporous channels and/or cages. The low-pressure portion of the isotherm indicated the existence of micropores (El-Sheikh et al. 2009b). The average pore diameter of samples heated at 400 °C was approximately 2–6 nm, as seen in Fig. 8b. Colmenares et al. (2014) reported that Cr_2O_3 was used as a photocatalyst for phenol degradation. The surface area of this photocatalyst material is about 5–10 m^2/g, when calcined from 180 to 600 °C. From the above results, the prepared Cr oxide should be a promising adsorbent and photocatalyst, especially as the material has nanosize dimensions, a mesoporous structure and a higher surface area (about 30 m^2 g^{-1}) than that reported by Colmenares et al. (2014).

Thermal behavior

The DTA and TGA data for Cr_2O_3 nanoparticles are graphically represented in Fig. 9. A weight loss is evident by the endothermic peak at 163 °C. The peak may be assigned to the release of hydroscopic water molecules (El-Sheikh et al. 2009a). However, heating Cr hydroxide samples to temperatures of 300–500 °C shows an exothermic peak at 433 °C corresponding to additional weight loss. This peak could be assigned to the decomposition of CrO_3 into Cr_2O_3 with oxygen liberation (Lime et al. 2006), which is consistent with XRD data:

$$4CrO_3 \rightarrow CrO_3 + 1{}^1\!/_2O_2 \quad (1)$$

Hypothetical model for the formation mechanism

The tannery waste solution contains metal ions such as Cr, Ca and Mg. It is, therefore, reasonable to separate the elements before disposal or recycling of the tannery waste effluent. This study aimed to use Ca and Cr ions for synthesis of Ca oxalate or sulfate and Cr oxide nanoparticles, respectively.

The element Cr has a body-centered cubic crystal structure with an atomic structure [Ar] $3d^5$ $4s^1$. The metal can exhibit a wide range of possible oxidation states in chemical compounds with the +3 and +6 states being the most common and with the former being the more stable energetically; compounds with oxidation states +1, +4 and +5 are rare. Like molybdenum, tungsten and rhenium, Cr has a special ability to form a quintuple bond, also known as a fivefold bond, which was first discovered in 2005. In Cr compounds, di-Cr was found to have a quintuple bond,

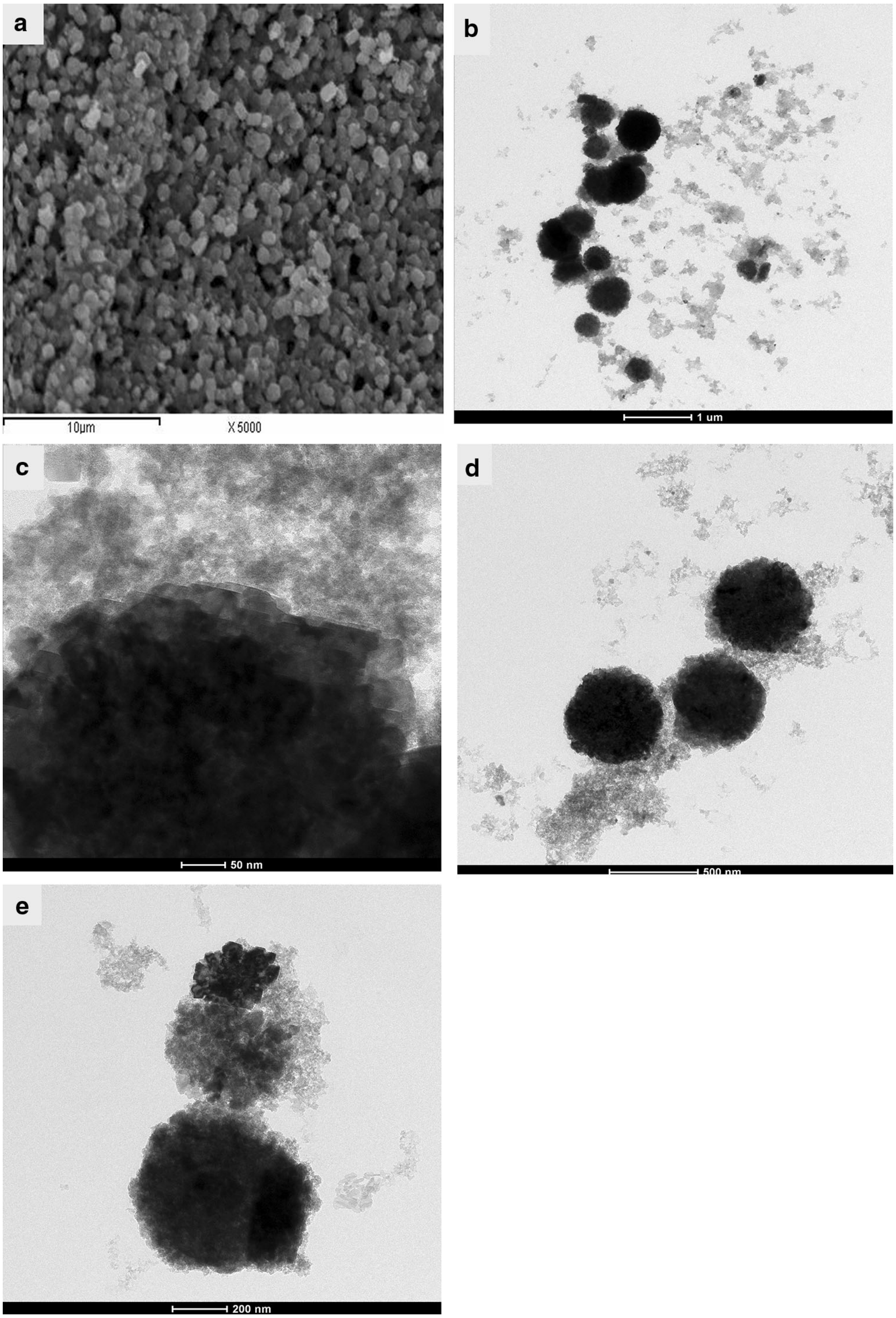

Fig. 7 **a** Micrographs of the chromium oxide mesospheres after heating at 500 °C. **b–e** TEM images for Cr_2O_3 samples heated at 400 and 500 °C

which means that 10 electrons are participating in the metal-to-metal bond. Chromium uses a terphenyl ligand to perform this action, thus making it relatively weak, but stable up to 200 °C. A quintuple bond is only possible if a Cr atom has only one other ligand to maintain bond stability. Although the discovery is fairly recent, it has already provided great insight into how transition metals are able to bond with each other (Greenwood et al. 1997). In terms of chemical properties, Cr hydroxide particles are amphoteric. With Cr hydroxide, three $(OH)^{-1}$ groups replace three hydronium molecules around the Cr atom to form the following configuration (Cañizares et al. 2006):

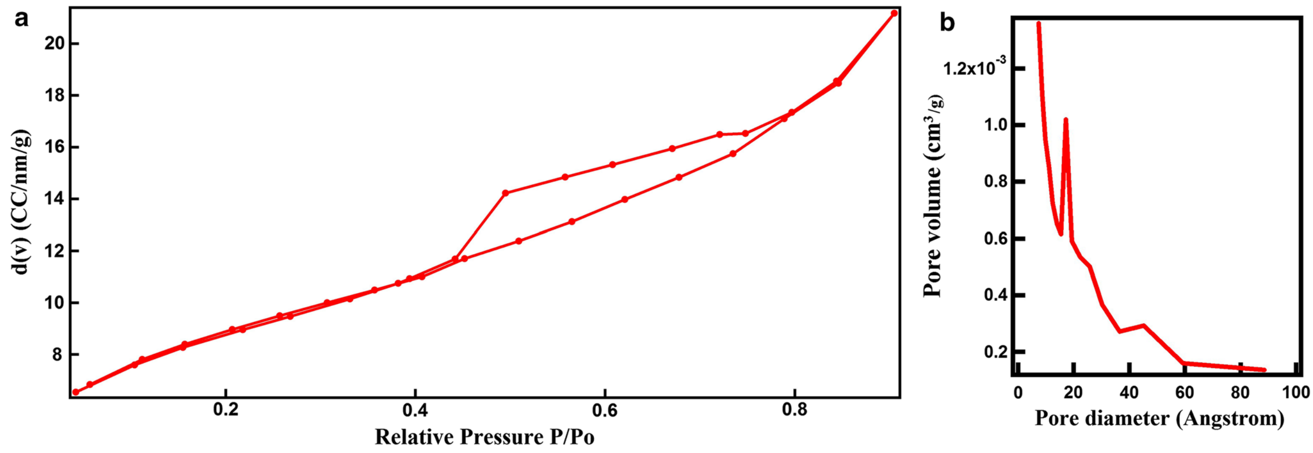

Fig. 8 **a–b** Nitrogen adsorption–desorption isotherm and pore size distribution for Cr_2O_3 nanoparticles (sample heated at 400 °C)

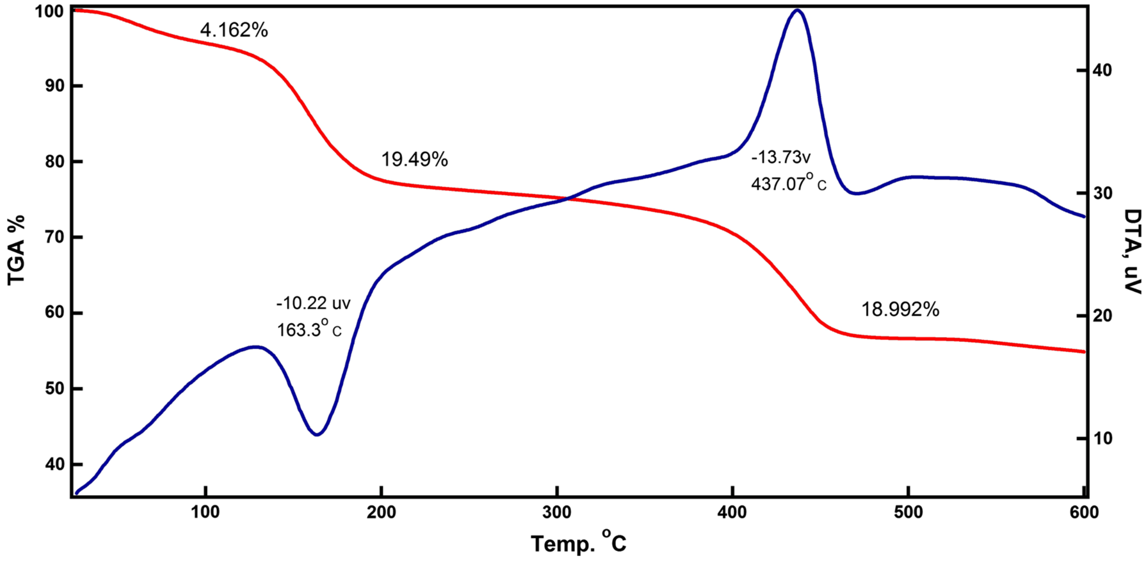

Fig. 9 TGA and DTA plots for Cr_2O_3 nanoparticles

$$[Cr(H_2O)_6]^{3+}_{(aq)} + 3OH^-_{(aq)} == > [Cr(OH)_3(H_2O)_3]_{(s)} + 3H_2O_{(1)} \qquad (2)$$

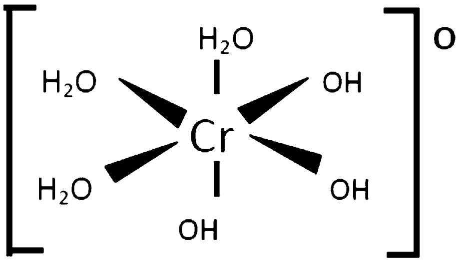

Water molecules establish a water film, which coats the Cr hydroxide molecule. When precipitated, Cr hydroxide molecules co-link together by weak adhesion forces under the surface tension action of the water coating. A nucleus for particle formation is thus initiated. Particle propagation takes place with a progressive weakness occurring in the adhesion forces of the particles so that they attain optimum size. Particles are not agglomerated on filtration hence can form a highly spongy gel-like structure. Heating this structure up to 400 °C involves degradation of the hydrated water, and $Cr(OH)_3$ decomposes to different forms of Cr oxide. It is worth noting that the Cr hydroxide precipitate produces nanoparticles of spongy amorphous Cr oxide when heated at 300 °C, which crystallizes upon further heating at 400 °C.

Conclusion

Chromium-rich effluent, generated from the leather tanning process was studied as a potential feedstock for generating Cr oxide nanoparticles. Preliminary separation of Ca and Cr ions in the waste effluent aided the synthesis of Ca oxalate and mesosphere Cr oxide nanoparticles. The physicochemical characteristics of the nanomaterial depended on the preparation conditions and parameters such as sample pH, heating temperature and time. The final product consisted of mesospheres built up from smaller nanoparticles. The smaller nanoparticles possess a large specific surface area and would constitute active centers suitable for catalyzation of microspheres. Results are explained on the premise that Cr metal has a special ability to form a quintuple bond. Heating such structures up to 400 °C involves degradation of the hydrated water, and the $Cr(OH)_3$ decomposes to Cr oxides of differing valences. The trivalent Cr oxide species, at 500 °C, has a mesoporous structure and a mesosphere shape. A mechanism for the formation of the spongy structure of the Cr oxide nanoparticles was proposed. It is of interest to note that the water remaining after removal of Ca and Cr ions was found to be suitable for recycling in the tannery process.

Acknowledgments The authors would like to thank the Central Metallurgical Research & Development Institute, Egypt, for financial support for this research (Grant No 954/D.M/2012).

References

Abreu MA, Toffoli SM (2009) Characterization of a chromium-rich tannery waste and its potential use in ceramics. Ceram Int 35:2225–2234. doi:10.1016/j.ceramint.2008.12.011

Brunauer S, Emmett PH, Teller E (1938) Adsorption of gases in multimolecular layers. J Am Chem Soc 60:309. doi:10.1021/ja01269a023

Beckhoff B, Kanngießer B, Langhoff N, Wedell R, Wolff H (2006) Handbook of practical X-ray fluorescence analysis, Springer, ISBN 3-540-28603-9

Cañizares P, Martínez F, Jiménez C, Lobato J, Rodrigo MA (2006) Comparison of the aluminum speciation in chemical and electrochemical dosing processes. Ind Eng Chem Res 45:8749–8756. doi:10.1021/ie060824a

Coats AW, Redfern JP (1963) Thermogravimetric analysis: a review. Analyst 88:906–924. doi:10.1039/AN9638800906

Colmenares JC, Lisowski P, Jose MB, Cot J, Rafael L (2014) Unprecedented photocatalytic activity of carbonized leather skin residues containing chromium oxide phases. Appl Catal B Environ 150–151:432–437. doi:10.1016/j.apcatb.2013.12.038

El-Sheikh SM, Rabbah M (2013) Novel low temperature synthesis of spinel nano-magnesium chromites from secondary resources. Thermochim Acta 568(20):13–19. doi:10.1016/j.tca.2013.06.024

El-Sheikh SM, Harraz FA, Abdel-Halim KS (2009a) Catalytic performance of nanostructured iron oxides synthesized by thermal decomposition technique. J Alloys Compd 487:716–723. doi:10.1016/j.jallcom.2009.08.053

El-Sheikh SM, Mohamed RM, Fouad OA (2009b) Synthesis and structure screening of nanostructured chromium oxide powders. J Alloys Compd 482:302–307. doi:10.1016/j.jallcom.2009.04.011

Gebrehawaria G, Hussen A, Rao VM (2014) Removal of hexavalent chromium from aqueous solutions using barks of Acacia albida and leaves of Euclea schimperi. Int J Environ Sci Technol. doi:10.1007/s13762-014-0530-2

Greenwood NN, Earnshaw A (1997) Chemistry of the elements, 2nd edn. Butterworth–Heinemann, New York, ISBN 0080379419

Gupta RK, Mitchell E, Candler J, Kahol PK, Ghosh K, Dong L (2014) Facile synthesis and characterization of nanostructured chromium oxide. Powder Technol 254:78–81. doi:10.1016/j.powtec.2014.01.014

International Union of Leather Technologists and Chemists Societies (IULTCS), IUE (2004) Assessment for chromium containing waste from the leather industry. In: International Union of Environment IUE, pp 1–4. http://www.iultcs.org/environment.asp

Jiao C, Cheng Y, Fan W, Li J (2014) Synthesis of agar-stabilized nanoscale zero-valent iron particles and removal study of hexavalent chromium. Int J Environ Sci Technol. doi:10.1007/s13762-014-0524-0

Kabir G, Ogbeide SE (2008) Removal of chromate in trace concentration using ion exchange from tannery wastewater. Int J Environ Res 2(4):377–384

Kanagaraj J, Babu NKC, Mandal AB (2008) Recovery and reuse of chromium from chrome tanning waste water aiming towards zero discharge of pollution. J Clean Prod 16:1807–1813. doi:10.4172/2155-6199.1000107

Kilic E, Fontb J, Puigb R, Olakc SC, Elik DC (2011) Chromium recovery from tannery sludge with saponin and oxidative remediation. J Hazard Mater 185:456–462. doi:10.1016/j.jhazmat.2010.09.054

Lime MD, Bonadimann R, de Andrade MJ, Toniolo JC, Bergmann CP (2006) Nanocrystalline Cr_2O_3 and amorphous CrO_3 produced by solution combustion synthesis. J Euro Ceram Soc 26:1213–1220. doi:10.1016/j.jeurceramsoc.2005.01.042

Ludvik J (2004) Chrome balance in leather processing, United Nations industrial development organization, US/RAS/92/120/11-51, Regional programme for pollution control in the tanning industry in south-east Asia, Report pp 1–18

Macchi G, Pagano M, Pettine M, Santori M, Tiravanti G (1991) A bench study on chromium recovery from tannery sludge. Wat Res 25:1019–1026. doi:10.1016/0043-1354(91)90152-G

Ortega LM, Lebrunb R, Nöelc IM, Hausler R (2005) Application of nanofiltration in the recovery of chromium (III) from tannery effluents. J Sep Purif Technol 44:45–52. doi:10.1016/j.seppur.2004.12.002

Patterson A (1939) The Scherrer Formula for X-Ray Particle Size Determination. Phys Rev 56:978–982

Scherrer P (1918) eund der Inneren Struktur von Röntgenstrahlen, Bestimmung der Gröss Kolloidteilchen Mittels Nachrichten von der Gesellschaft der Wissenschaften, Göttingen". Mathematisch-Physikalische Klasse 2:98–100

Song Z, Williams CJ, Edyvean RGJ (2004) Treatment of tannery wastewater by chemical coagulation. Desalination 164:249–259. doi:10.1016/S0011-9164(04)00193-6

Sumathi KMS, Mahimairaja S, Naidu R (2005) Use of low-cost biological wastes and vermiculite for removal of chromium from tannery effluent. Bioresour Technol 96:309–316. doi:10.1016/j.biortech.2004.04.015

Tahir SS, Naseem R (2007) Removal of Cr(III) from tannery wastewater by adsorption onto bentonite clay. Sep Purif Technol 53:312–321. doi:10.1016/j.seppur.2006.08.008

Terzyk AP, Wloch J, Furmaniak S, Kowalczyk P, Harris PJF, Rychlicki G, Gauden PA (2007) How realistic is the pore size distribution calculated from adsorption isotherms if activated carbon is composed of fullerene-like fragments? Phys Chem Chem Phys 9:5919–5927

Williams DB, Carter CB (1996) Transmission electron microscopy: a textbook for materials science, Volume 2. Springer. p. 559. ISBN 0-306-45324-X

Zhou S, Zhou LX, Wang SM, Fang D (2006) Removal of Cr from tannery sludge by bioleaching method. J Environ Sci 18:885–890. doi:10.1016/S1001-0742(06)60009-0

Zhu LUZ, Yao X, Lu G, Yan Z (2008) Synthesis and characterization of chromium oxide nanocrystals via solid thermal decomposition at low temperature. Microporous Mesoporous Mater 112:621–626. doi:10.1016/j.micromeso.2007.10.044